

Electrical Properties of Intercalated Conducting Polymer Nanocomposites

A DEY

Department of Chemistry, Sarsuna College, Kolkata 700061, India
Corresponding author: deyashis@gmail.com (Ashis Dey).

Abstract

The synthesis of conducting polymers (CP) by encapsulating into inorganic materials is a fascinating field in nanomaterials [1,2]. The incorporation is usually done in mesoporous, microporous, crystalline and amorphous solids, which are used as host materials for the conducting polymers. The encapsulation protects CP from atmosphere and also chemical attack. The most advantageous is that it eliminates interchain interactions of polymers. This enables to study the electronic properties and charge transport mechanisms of an isolated polymer chain. The addressing of individual chain leads to potential applications in molecular electronics. The incorporation of polymer is generally done by two ways: one is insertion of preformed polymer in the host and the other is polymerization within the layers of host. Nanocomposites of conducting polyaniline and xerogels are synthesized by redox intercalation technique. Polyaniline of molecular size 5 Å is formed within the interlamellar space of gels. The contribution to dc conductivity is mainly from polyaniline. The intercalation is confirmed by the observation of lattice expansion of V₂O₅ xerogel. Dc conductivity of the gel follows Arrhenius type temperature dependence while the nanocomposites exhibit three dimensional variable range hopping.

Keywords: intercalation, polyaniline, variable range hopping.

Introduction

Vanadium oxides and their related compounds have been investigated both extensively and intensively due to their novel physicochemical properties and potential applications in lithium batteries,¹ electric field-effect transistors²⁻⁴ and chemical sensors.^{5,6} The layered structure and redox ability of vanadium oxides allow the insertion of various guest species such as polymers, leading to the formation of hybrid materials with a mixed valence of vanadium (V⁴⁺/V⁵⁺).⁷ Organic-inorganic hybrid structures have been designed to achieve new materials with improved properties because of the synergic effects of their constituents at a molecular level.^{8,9} Specifically, the intercalation of conducting polymers into layered inorganic

hosts has been a topic of research interest over the past half century.¹⁰⁻¹³ Among the family of conducting polymers, polyaniline is of great interest because its electrical and optical properties can be controlled by a simple and reversible acid-base doping-dedoping process.¹⁴

Intercalative polymerization of conducting polymers inside the layered structures needs substantial oxidizing power. Among layered materials namely, FeOCl^{15,16}, V₂O₅^{17,18} and α -RuCl₃¹⁹ are suitable for the postintercalation polymerization. Crystalline vanadium pentoxide has sufficiently strong oxidizing power among the high oxidation transition metal oxides. The intercalation of small ions are only possible due to strong interlayer bonding interactions. The vanadium pentoxide xerogel as represented by

$V_2O_5 \cdot nH_2O$ are layered materials with water in the interlayer space²⁰. The distance between two layers depend on the amount of intercalated water. Water molecule is very weakly hydrogen bonded to the oxide network. Vanadium pentoxide xerogel with higher interlayer distance is suitable for intercalation of a variety of guest specimen. The intercalation of polyaniline (PANI)¹⁷, polypyrrole (PPY), polyethylene oxide (PEO)^{21,22} polyethylene dioxythiophene (PEDOT)²³ in V_2O_5 have been performed. Redox intercalation modifies the electronic structure of host material V_2O_5 both by expanding the interlayer distance and changing the electronic configuration of V^{5+} ions. During the polymerization process V^{5+} transfers to V^{4+} which yields mixed valence behavior of V atoms.

Experimental

Preparation of $V_2O_5 \cdot nH_2O$ Xerogel

The preparation of $V_2O_5 \cdot nH_2O$ xerogel has been followed as described by Lemerle et al.²³. In a typical synthesis, 2 gm of sodium metavanadate is dissolved in 125 ml of deionized water. The resulting solution is passed through a H^+ ion exchanger column, packed with 15 gm of resin (Dowex-50X2, 200-400) forming a pale orange solution of HVO_3 . Aqueous HVO_3 solution is then dried in air at room temperature, which is polymerized to a red V_2O_5 xerogel (sample S1) within few days. After evaporation of excess water dark red film is formed and it is grounded to powder for subsequent use.

Preparation of $(PANI)_x V_2O_5 \cdot nH_2O$

Two different composites (sample S2 and S3) are prepared with different amount of aniline and $V_2O_5 \cdot nH_2O$ xerogel. 0.5 ml and 1 ml aniline are dispersed in 20 ml deionized water for sample S2 and S3 respectively, followed by addition of 0.5 gm of V_2O_5 xerogel in each case. The mixture

is allowed to stand at room temperature for 5 h in air. The product is isolated by centrifugation, washed with acetone and dried in vacuum at room temperature. Green powder obtained is then pressed to form pellet and used for characterizations and transport measurements. The X-ray powder diffraction studies are carried out with Philips Diffractometer (PW1710) in the range $2-40^\circ$ using $Cu-K_\alpha$ radiation. Fourier transform infrared (FTIR) spectra are recorded from pressed KBr pellets using a Perkin-Elmer-1600 FTIR spectrometer.

Results and discussion

The water content and the composition of material $(PANI)_x V_2O_5 \cdot nH_2O$ are determined by the elemental carbon, hydrogen and nitrogen (CHN) analyzer. The percentages of C, H, N and the values of x and n for different samples are shown in Table 1. The actual C/N=6 ratio in PANI ($-C_6H_4NH-$) is almost maintained in all the composites. The amount of intercalated water in xerogel is 1.97 and it decreases with intercalation of polyaniline (PANI). This indicates that PANI is formed within the layers of gel through the replacement of water.

The X-ray diffraction (XRD) patterns of $V_2O_5 \cdot nH_2O$ and the composites are shown in Figure 1. The first peak in Figure 1a indicates (001) reflections. The interlayer distance in the (001) direction is estimated from Bragg's law, $2d \sin \theta = \lambda$. The layer spacing of gel with 1.97 H_2O is 12.10 Å. The first peak in Figure 1b shifts to lower angle which corresponds to the lattice expansion from 12.10 Å to 13.87 Å due to the intercalation of PANI. The maximum lattice expansion for $x = 0.77$ is 3.72 Å. The intercalation of PANI occurs through removal of water layer which is about 2.8 Å. The real lateral size of PANI molecule is around 5 Å.

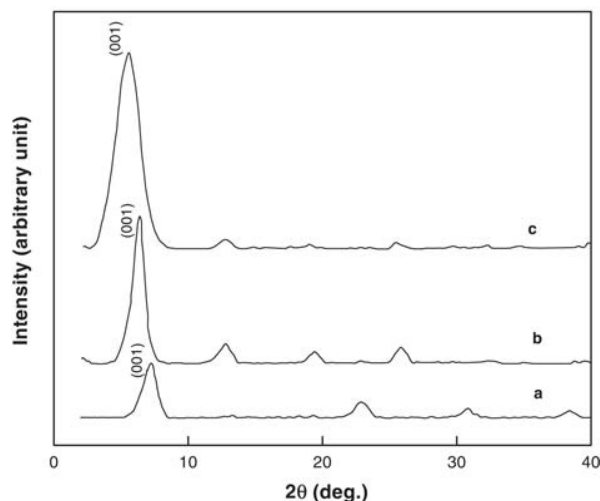


Fig 1: X-ray diffraction pattern of (a) $V_2O_5 \cdot 1.97H_2O$, (b) $(PANI) 0.64V_2O_5 \cdot 0.11H_2O$ (c) $(PANI) 0.77V_2O_5 \cdot 0.06H_2O$

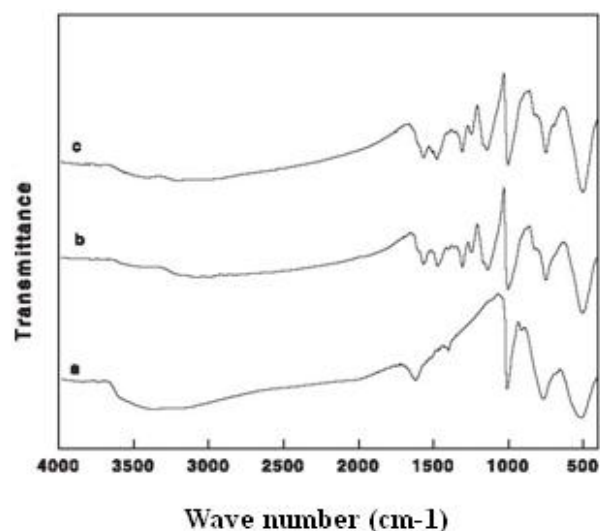


Fig 2: Fourier Transform Infrared (FTIR) spectra of (a) $V_2O_5 \cdot 1.97H_2O$, (b) $(PANI) 0.64V_2O_5 \cdot 0.11H_2O$ (c) $(PANI) 0.77V_2O_5 \cdot 0.06H_2O$.

The FTIR spectra of the gel and the nanocomposites are shown in Figure 2. The absorptions at 764 and 517 cm^{-1} are for V-O-V stretching modes and 1010 cm^{-1} is for V=O stretching. The spectra of the nanocomposites reveal the bands $1000\text{--}508\text{ cm}^{-1}$ corresponding to V_2O_5 and $1600\text{--}1100\text{ cm}^{-1}$ characteristic of

PANI. The bands 1590 , 1487 cm^{-1} originate from C-C ring stretching and 1307 cm^{-1} from C-H bending or C-N stretching of PANI. The identical XRD and FTIR spectra except the small changes in the peaks indicate the existence of layered structure of $V_2O_5 \cdot nH_2O$ after intercalation. The room temperature dc conductivity $\sigma_{dc}(RT)$ of the gel is $5.08 \times 10^{-6}\text{ S/cm}$ and that of sample S3 is $1.97 \times 10^{-3}\text{ S/cm}$. Intercalation of PANI into gel enhances the conductivity by about 1000 times throughout the composition range. The increase of conductivity with PANI concentration is due to the formation of more conducting PANI in the network of oxide gel and the increase of polymer chain length. The temperature dependence of $\ln \sigma_{dc}(T)$ of sample S1 is shown in Figure 3.

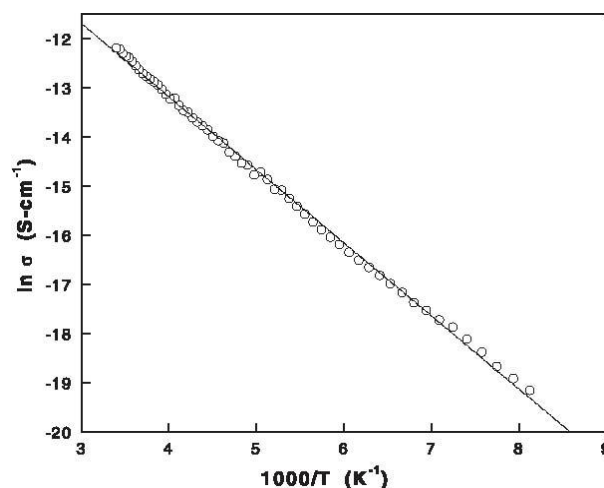


Fig 3: Temperature variation of dc conductivity of V_2O_5 xerogel.

The straight line of $\ln \sigma_{dc}(T)$ vs. $1/T$ suggests that thermally activated conduction process occurs. Thus the conductivity as a function of temperature can be represented by the relation,

$$\sigma(T) = \sigma_a \exp(-E/kT) \quad (1)$$

where E is the activation energy and k is the Boltzmann constant. The estimated value of E is 0.13 eV .

The variation of dc conductivity with temperature for the nanocomposites (S2 and S3) are shown in Figure 4. The linear behavior of $\ln \sigma_{dc}(T)$ with $T^{-1/4}$ indicates that $\sigma_{dc}(T)$ follows three dimensional variable range hopping (VRH) model²⁴,

$$\sigma(T) = \sigma_0 \exp(-(T_0/T)^{1/4}). \quad (2)$$

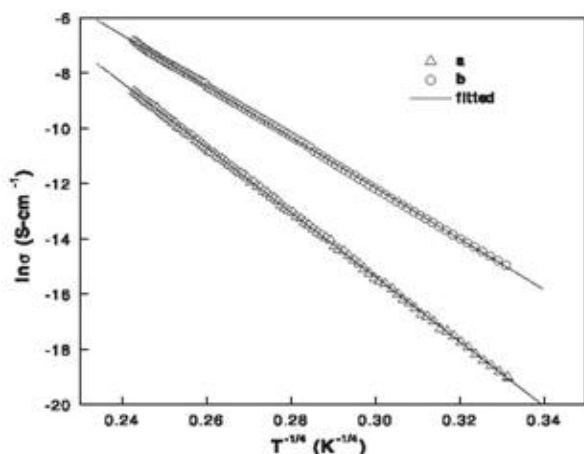


Fig 4: Variable-temperature dc conductivity for two nanocomposites

(a) (PANI) 0.64V₂O₅.0.11H₂O

(b) (PANI)0.77V₂O₅.0.06H₂O

The characteristic temperature $T_0 = 16/(kL^3N(E_F))$, where L is the localization length and $N(E_F)$ is the density of states at the Fermi level. The slopes of straight lines in Figure 4 give the values of $T_0 = 18.74 \times 10^7$ K of S2 and 7.20×10^7 K of S3. The smaller value of T_0 i.e. the larger of L suggests that sample S3 is more conductive than that of S2.

The incorporation of PANI into V₂O₅ induces V⁴⁺ ions during redox reaction. The formation of V⁴⁺ with d1 conduction electrons gives semiconducting behavior. Electric conduction in the oxide network is due to hopping of electrons from V⁴⁺ sites to V⁵⁺. Electrical conduction in PANI arises from the delocalized π electrons along the backbone of polymer. The intercalated PANI leads to two different types of conduction

processes. Pure gel reveals thermally activated type conduction while the nanocomposites show VRH type conduction. Thus confined PANI in the nanocomposites plays an important factor in dc conduction process. Electrons are responsible for dc conduction in the nanocomposites.

Conclusion

Physical properties of nanocomposites depend on oxide, water and conducting PANI phases. Intercalation of PANI increases V⁴⁺ ions and decrease water molecule. Nano confinements of PANI within the interlayer space of oxide drastically modify the chain length, conformation and orientation. Moreover interchain interaction is minimized and it is only possible via oxide layers due to the formation of monolayer of PANI. Molecular interaction among PANI, oxide layer and water yield the actual transport properties. The displacements of charge carriers become shorter with the increase of frequency. As a result of it a correlated motion occurs which lead to a strong interaction among the different kinds of charge carriers.

References

- [1] Y. Wang and G. Z. Cao, *Chem. Mater.*, 2006, **18**, 2787.
- [2] G. T. Kim, J. Muster, V. Krstic, J. G. Park, Y. W. Park, S. Roth and M. Burghard, *Appl. Phys. Lett.*, 2000, **76**, 1875.
- [3] J. Muster, G. T. Kim, V. Krstic, J. G. Park, Y. W. Park, S. Roth and M. Burghard, *Adv. Mater.*, 2000, **12**, 420.
- [4] P. R. Somani, R. Marimuthu and A. B. Mandale, *Polymer*, 2001, **42**, 2991.
- [5] G. Gu, M. Schmid, P. W. Chiu, A. Minett, J. Fraysse, G. T. Kim, S. Roth, M. Kozlov, E. Munoz and R. H. Baughman, *Nat. Mater.*, 2003, **2**, 316.

- [6] L. Biette, F. Carn, M. Maugey, M. F. Achard, T. Maquet, N. Steunou, T. Livage, H. Serier and R. Backov, *Adv. Mater.*, 2005, **17**, 2970.
- [7] T. Chirayil, P. Y. Zavalij and M. S. Whittingham, *Chem. Mater.*, 1998, **10**, 2629.
- [8] A. Sellinger, P. M. Weiss, A. Nguyen, Y. F. Lu, R. A. Assink, W. L. Gong and C. J. Brinker, *Nature*, 1998, **394**, 256.
- [9] K. Yamamoto, Y. Sakata, Y. Nohara, Y. Takahashi and T. Tatsumi, *Science*, 2003, **300**, 470.
- [10] P. Gomez-Romero, *Adv. Mater.*, 2001, **13**, 163.
- [11] G. Yang, W. H. Hou, Z. Z. Sun and Q. J. Yan, *J. Mater. Chem.*, 2005, **15**, 1369.
- [12] G. Yang, W. H. Hou, X. M. Feng, X. F. Jiang and J. Guo, *Adv. Funct. Mater.*, 2007, **17**, 3521.
- [13] G. Yang, W. H. Hou, X. M. Feng, L. Xu, Y. G. Liu, G. Wang and W. P. Ding, *Adv. Funct. Mater.*, 2007, **17**, 401.
- [14] W. S. Huang, B. D. Humphrey and A. G. Macdiarmid, *J. Chem. Soc., Faraday Trans. 1*, 1986, **82**, 2385.
- [15] M.G. Kanatzidis, C.-G. Wu, H.O. Marcy, C.R. Kannewurf, *Adv. Mater.* **2**, 364 1990
- [16] S.R. Hwang, W.-H. Li, K.C. Lee, J.W. Lynn, C.-G. Wu, *Phys. Rev. B.* **62**, 14157 (2000)
- [17] C.-G. Wu, D.C. DeGroot, H.O. Marcy, J.L. Schindler, C.R. Kannewurf, Y.-J. Liu, W. Hirpo, M.G. Kanatzidis, *Chem. Mater.* **8**, 1992 (1996)
- [18] M.G. Kanatzidis, C.-G. Wu, H.O. Marcy, C.R. Kannewurf, *J. Am. Chem. Soc.* **111**, 4139 (1989)
- [19] L. Wang, P. Brazis, M. Rocci, C.R. Kannewurf, M.G. Kanatzidis, *Chem. Mater.* **10**, 3298 (1998)
- [20] J. Livage, *Chem. Mater.* **3**, 578 (1991)
- [21] Y.-J. Liu, J.L. Schindler, D.C. DeGroot, C.R. Kannewurf, W. Hirpo, M.G. Kanatzidis, *Chem. Mater.* **8**, 525 (1996)
- [22] Y.-J. Liu, D.C. DeGroot, J.L. Schindler, C.R. Kannewurf, M.G. Kanatzidis, *Chem. Mater.* **3**, 992 (1991)
- [23] J. Lemerle, L. Nejem, J. Lefebvre, *J. Inorg. Nucl. chem.* **42**, 17 (1980)
- [24] N.F. Mott, E. Davis, *Electronic Process in Non Crystalline Materials*, 2nd edn. (Oxford, Clarendon, 1979)